DEUTSCHES ELEKTRONEN – SYNCHROTRON

DESY 91-092
August 1991

Measurement of R and Determination of the Charged-Particle Multiplicity in e^+e^- Annihilation at $\sqrt{s}$ around 10 GeV

The ARGUS Collaboration

ISSN 0418-9833

NOTKESTRASSE 85 · D-2000 HAMBURG 52

To be sure that your preprints are promptly included in the
HIGH ENERGY PHYSICS INDEX,
send them to the following (if possible by air mail):

DESY
Bibliothek
Notkestrasse 85
D–2000 Hamburg 52
Germany

DESY 91-092
August 1991

ISSN 0418-9833

Measurement of R and Determination of the Charged-Particle Multiplicity in e^+e^- Annihilation at $\sqrt{s}$ Around 10 GeV

The ARGUS Collaboration

H. Albrecht, H. Ehrlichmann, T. Hamacher, A. Krüger, A. Nau, A. Nippe, M. Reidenbach, M. Schäfer, H. Schröder, H. D. Schulz, F. Sefkow, R. Wurth
DESY, Hamburg, Germany

R. D. Appuhn, C. Hast, G. Herrera, H. Kolanoski, A. Lange, A. Lindner, R. Mankel, M. Schieber, T. Siegmund, B. Spaan, H. Thurn, D. Töpfer, A. Walther, D. Wegener
Institut für Physik[1], Universität Dortmund, Germany

M. Paulini, K. Reim, U. Volland, H. Wegener
Physikalisches Institut[2], Universität Erlangen-Nürnberg, Germany

M. Hapke, R. Mundt, T. Oest, W. Schmidt-Parzefall
II. Institut für Experimentalphysik, Universität Hamburg, Germany

W. Funk, J. Stiewe, S. Werner
Institut für Hochenergiephysik[3], Universität Heidelberg, Germany

S. Ball, J. C. Gabriel, C. Geyer, A. Hölscher, W. Hofmann, B. Holzer, S. Khan, K. T. Knöpfle, J. Spengler
Max-Planck-Institut für Kernphysik, Heidelberg, Germany

D. I. Britton[4], C. E. K. Charlesworth[5], K. W. Edwards[6], H. Kapitza[6], P. Krieger[5], R. Kutschke[5], D. B. MacFarlane[4], R. S. Orr[5], P. M. Patel[4], J. D. Prentice[5], S. C. Seidel[5], Y. Tsipolitis[4], E. Tzamariudaki[4], R. G. Van de Water[5], T.-S. Yoon[5]
Institute of Particle Physics[7], Canada

D. Reßing, S. Schael, K. R. Schubert, K. Strahl, R. Waldi, S. Weseler
Institut für Experimentelle Kernphysik[8], Universität Karlsruhe, Germany

B. Boštjančič, G. Kernel, P. Križan, E. Križnič, T. Podobnik, T. Živko
Institut J. Stefan and Oddelek za fiziko[9], Univerza v Ljubljani, Ljubljana, Slovenia

H. I. Cronström, L. Jönsson
Institute of Physics[10], University of Lund, Sweden

V. Balagura, M. Danilov, A. Droutskoy, B. Fominykh, A. Golutvin, I. Gorelov, F. Ratnikov, V. Lubimov, A. Rostovtsev, A. Semenov, S. Semenov, V. Shevchenko, V. Soloshenko, I. Tichomirov, Yu. Zaitsev
Institute of Theoretical and Experimental Physics, Moscow, USSR

R. Childers, C. W. Darden
University of South Carolina[11], Columbia, SC, USA

[1] Supported by the German Bundesministerium für Forschung und Technologie, under contract number 054DO51P.
[2] Supported by the German Bundesministerium für Forschung und Technologie, under contract number 054ER12P.
[3] Supported by the German Bundesministerium für Forschung und Technologie, under contract number 055HD21P.
[4] McGill University, Montreal, Quebec, Canada.
[5] University of Toronto, Toronto, Ontario, Canada.
[6] Carleton University, Ottawa, Ontario, Canada.
[7] Supported by the Natural Sciences and Engineering Research Council, Canada.
[8] Supported by the German Bundesministerium für Forschung und Technologie, under contract number 054KA17P.
[9] Supported by the Department of Science and Technology of the Republic of Slovenia and the Internationales Büro KfA, Jülich.
[10] Supported by the Swedish Research Council.
[11] Supported by the U.S. Department of Energy, under contract DE-AS09-80ER10690.

Abstract. We have measured the R value in non-resonant e^+e^- annihilation using the ARGUS detector at the storage ring DORIS II. At a centre-of-mass energy $\sqrt{s} = 9.36$ GeV the ratio of the hadronic cross-section to the μ-pair cross-section in lowest order QED has been determined to be $R = 3.46 \pm 0.03 \pm 0.13$. In addition, we have measured the charged-particle multiplicities in non-resonant hadron production at $\sqrt{s} = 10.47$ GeV just below the $B\overline{B}$ threshold and in $\Upsilon(4S)$ resonance decays. For the average charged-particle multiplicities in continuum events and $\Upsilon(4S) \to B\overline{B}$ decays we obtain $\langle n \rangle_{cont} = 8.35 \pm 0.02 \pm 0.20$ and $\langle n \rangle_{\Upsilon(4S)} = 10.81 \pm 0.05 \pm 0.23$.

1 Introduction

The R value is defined as the ratio of the non-resonant hadronic cross-section to the Born cross-section for μ-pair production

$$R = \frac{\sigma^0(e^+e^- \to hadrons)}{\sigma^0(e^+e^- \to \mu^+\mu^-)} \quad , \tag{1}$$

where the symbol σ^0 indicates that the effects of higher order QED corrections are removed. In the quark parton model the R value measures the sum of the squares of the quark charges times the color factor $N_c = 3$. Deviations from the simple quark model prediction are expected from higher order QCD corrections including gluon bremsstrahlung and gluon vertex corrections. At centre-of-mass energies far below the Z^0 mass, where electroweak contributions to the R value are negligible, the R value in second order QCD is given by

$$R = 3 \sum_{i=1}^{n_f} Q_i^2 \times \{ \ 1 \ + C_1 \cdot (\frac{\alpha_s}{\pi}) \ + C_2 \cdot (\frac{\alpha_s}{\pi})^2 \ \} \ . \tag{2}$$

The coefficients C_1 and C_2 are given in the $\overline{\mathrm{MS}}$ renormalization scheme by $C_1 = 1$ and $C_2 = 1.986 - 0.115\, n_f$, where n_f denotes the number of open quark flavours. The third order QCD correction $O(\alpha_s^3)$ is still not known, since the published calculations [1] were shortly afterwards found to be incorrect [2].

A measurement of R at an energy well above the charm threshold and below the Υ resonances is suited to determine the strong coupling constant α_s. This is based on the fact that in this energy region the QCD corrections to R are assumed to be small enough to apply perturbation theory and large enough to be measurable.

In the following we present a measurement of R at a centre-of-mass energy of $\sqrt{s} = 9.36$ GeV. From the experimental side, the determination of R requires a good separation of the hadron production in e^+e^- annihilation from other processes like τ-pair production and two-photon reactions. Therefore, the applied event selection procedure is also well suited to study and to determine the charged-particle multiplicity distributions in high statistics data samples of non-resonant hadron production and in $\Upsilon(4S) \to B\overline{B}$ decays.

2 Data Samples and Event Selection Procedure

The analyzed data were taken with the ARGUS detector at the e^+e^- storage ring DORIS II at a centre-of-mass energy of $\sqrt{s} = 9.36\,\mathrm{GeV}$ below the $\Upsilon(1S)$ resonance, in the continuum between 10.43 GeV and 10.54 GeV, and on the $\Upsilon(4S)$ resonance. The corresponding integrated luminosities are $8.3\,pb^{-1}$ and $35\,pb^{-1}$ for the two continuum data sets, and $95\,pb^{-1}$ for the $\Upsilon(4S)$ data sample. The integrated luminosity is measured from large angle Bhabha scattering. The error on the luminosity measurement is dominated by systematic effects and amounts to 1.8%, which is due to theoretical uncertainties in calculating the Bhabha cross-section of 1.0% and a 1.4% error on the efficiency determination [3]. A detailed description of the ARGUS detector, its trigger and particle identification capabilities can be found in Ref. [4].

Hadronic events were preselected by requiring at least three charged tracks with either a common vertex or an energy deposition of at least 1.7 GeV in the shower counters. The resulting event sample still contains considerable background from radiative Bhabha scattering, τ-pair production, two-photon reactions, and beam-gas and beam-wall interactions. Radiative Bhabha events with converted photons are almost completely removed from the event sample by cutting on the sum E_{12} of the observed shower energies of the two particles with the largest momenta and on an isolated-track-angle α discriminating between the topologies of radiative Bhabha events and two-jet like hadronic events. This angle is defined by first calculating for each track or photon the smallest opening angle with respect to all other particles. Choosing the largest one among these angles results in almost 180 degrees for radiative Bhabha events, whereas less than 90 degrees is typically obtained for $q\bar{q}$ and $B\overline{B}$ events. The cut is indicated by the solid line shown in Fig. 1, where we have plotted $\cos\alpha$ versus $E_{12}/\sqrt{s}$ for part of our continuum data. Events with entries in the upper-left part of the scatter-plot are accepted.

Beam related background as well as background from two-photon reactions is efficiently suppressed by requiring

$$\lambda = \sum |\vec{p}|/\sqrt{s} \; - \; 0.4 \; - \; 2.5 \cdot (\sum p_z/\sqrt{s})^2 \; > \; 0\,, \tag{3}$$

where $\vec{p}$ denotes the particle momentum vector and p_z its momentum component along the beam axis. The sums include the momenta of all charged particles and photons in an event and are normalized to the centre-of-mass energy. In Fig. 2 we plot $P_{sum} = \sum |\vec{p}|/\sqrt{s}$ versus $P_z = \sum p_z/\sqrt{s}$ for part of our continuum data at $\sqrt{s} = 9.36\,\mathrm{GeV}$. Again the solid line indicates the applied cut. Events with entries above the line are accepted.

3 Determination of R

3.1 Background Estimation

After these cuts the continuum sample at $\sqrt{s} = 9.36\,\mathrm{GeV}$ consists of 28969 events. Remaining possible background in our final continuum data originates from beam-gas and beam-wall interactions, τ-pair production, and two-photon reactions. The contamination from beam-gas and beam-wall reactions is negligible. This was estimated by studying the acceptance behaviour of our selection criteria for those events with vertex positions outside the nominal interaction region and extrapolating to the number of events with vertices inside the accepted vertex region.

From Monte Carlo simulations including initial-state radiation in the reaction $e^+e^- \to \tau^+\tau^-$ we estimate a contribution of $(3.7 \pm 0.8)\%$ from τ-pair production to the final event sample. The background from two-photon events was obtained from Monte Carlo simulations of various two-photon reactions with multi-pion final-states. After all selection criteria there remains a contribution of $(1.1 \pm 1.0)\%$ of two-photon background in our event sample. The large error on this contribution originates from the large uncertainty in the absolute scale of the cross-section for the simulated reactions.

In total, we obtain a background contribution of $(4.8 \pm 1.3)\%$ to our final continuum data sample used for the R determination. After background subtraction there remain $27578 \pm 170 \pm 377$ events, where the first error is statistical and the second systematic.

3.2 Radiative Corrections and Acceptance Calculation

From the number of background corrected hadronic events N_{ev} the R value is derived from the expression

$$R = \frac{N_{ev}}{\epsilon(1+\delta)\mathcal{L}} \cdot \frac{1}{\sigma^0_{\mu\mu}}\,, \tag{4}$$

where $\mathcal{L}$ denotes the integrated luminosity of the analyzed data sample, ϵ is the acceptance of our applied event selection procedure, and $\sigma^0_{\mu\mu} = 4\pi\,\alpha^2/3s$ is the Born cross-section for μ-pair production. Radiative corrections to the reaction $e^+e^- \to q\bar{q} \to$ *hadrons* are taken into account by the factor $(1 + \delta)$, which relates the Born cross-section σ^0 for hadron production to the measured cross-section

$$\sigma = \sigma^0(1+\delta) = \sigma^0(1 + \delta_{soft} + \delta_{vertex} + \delta_{vac} + \delta_{hard})\,. \tag{5}$$

The correction term $(1+\delta)$ receives contributions from *soft* and *hard* initial-state radiation, *vertex* corrections, and from *vacuum* polarization terms with lepton (e, μ, τ) and quark loops. The correction term for hard photon radiation shows a steep rise if the photon energy approaches its kinematic limit of $k_{max} = \sqrt{s}(1 - 4m_\pi^2/s)$ at the threshold for $\pi\pi$

production and depends on the modelling of the hadronic cross-section at low centre-of-mass energies. The latter is uncertain due to low lying resonances, like ρ and ω, and quark-pair production thresholds. However, this strong increase of the radiative corrections at large photon energies is fairly well compensated by the fact that the acceptance for events with hard bremsstrahlung photons, which are preferentially emitted along the beam axis, is small, well below 1/10 of the average acceptance. Thus, the product of ϵ and $(1+\delta)$ is stable against changes of the parametrization of the hadronic cross-section at low s values.

To determine the radiative corrections to the hadronic cross-section and the acceptance quantitatively, $q\bar{q}$ events were generated with the LUND-JETSET 6.3 program [5] and passed through a complete detector simulation. For initial-state radiation of soft photons a cut-off was applied at 1% of the beam energy. For the product $\epsilon \cdot (1+\delta)$ we obtain a value of 0.972 ± 0.027. The error on this product is mainly systematic and originates from neglecting higher order QED contributions to the radiative corrections (1.0%), from uncertainties in the hadronic part of the vacuum polarization correction (0.3%) and in the Monte Carlo calculation of the event selection efficiency (2.5%). This error includes uncertainties in modelling the detector response (1.5%) and in the hadronisation model used (2%). The systematic error on the long time stability (1.1%) of the detector response has been derived from continuum data at centre-of-mass energies arround 10.45 GeV, which have been recorded over a time period of 6 years. We have also studied the effect of different parametrizations for the hadronic cross-section at low s values on the radiative correction term and on the acceptance by replacing a simple $1/s$ dependence of $\sigma^0(e^+e^- \to hadrons)$ by a parametrization which includes low lying resonances and quark-pair production thresholds. This yields a systematic change in $\epsilon(1+\delta)$ of only 0.2%.

3.3 Results of R Measurement

Inserting in eq. 4 the background subtracted number of events, the integrated luminosity, the derived product of the selection efficiency ϵ and the radiative correction factor $(1+\delta)$, and dividing by the Born cross-section for μ-pair production results in a R value at $\sqrt{s} =$ 9.36 GeV of

$$R = 3.46 \pm 0.03 \pm 0.13 \ ,$$

where the first error is statistical and the second is systematic. The statistical error consists of the quadratic sum of 0.3% statistical uncertainty in the luminosity measurement and of 0.6% statistical error on the number of observed hadronic events. The systematic error on R includes the following contributions in quadrature: a relative uncertainty of 1.8% in the luminosity determination, 2.7% systematic error for the correction factor $\epsilon \cdot (1+\delta)$, a contribution of 1.3% for the uncertainty in the background determination, an error of 1.1% on the long time stability of the detector response, and an error of 1% due to the

effect on R by varying the cut parameters of the event selection criteria.

In Table 1 we compare our result on R with previous measurements of other experiments at similar centre-of-mass energies. Our result is the most precise one. However, all R measurements are dominated by systematic uncertainties. Forming the weighted average of the measurements in Table 1 results in a value of $R = 3.51 \pm 0.08$ at $\sqrt{s} \approx 10\,GeV$, where we have added the statistical and systematic errors quadratically. From eq. 2 with the number of open quark flavours $n_f = 4$, we obtain for the corresponding α_s a value of 0.155 ± 0.065. The error on α_s is dominated by systematic uncertainties and is still too large to allow a precise determination of the QCD scaling parameter $\Lambda_{\overline{MS}}$.

4 Study of Charged-Particle Multiplicity

4.1 Data Selection

We have used the selection criteria outlined in section 2 to study the charged-particle multiplicity distributions in our high statistics data samples of non-resonant hadron production at a centre-of-mass energy of 10.47 GeV and of $\Upsilon(4S) \to B\overline{B}$ decays. An additional cut was used to further suppress background from τ-pair events. It is illustrated in Fig. 3, which shows a scatter plot of the event topology parameter 'thrust' versus the isolated-track-angle α_{ch} as described in section 2, but using charged tracks only. τ-pair events with 1-3 topology populate the lower right corner, those with 3-3 topology the upper right corner. Their contribution is considerably reduced by rejecting all events to the right of the solid line shown in the Figure. Although the overall background in our event samples is less than 2% after all cuts, its contribution to event classes of low multiplicity is considerable. To estimate the background in each multiplicity class we slightly modified the cut of eq. 3 and compare the λ-distribution for each event class of the data to the corresponding one of Monte Carlo generated $q\bar{q}$-events. In Fig. 4 both distributions are shown for continuum events of observed multiplicity 4. The integrated difference between the distributions of real and Monte Carlo data for $\lambda > 0$ is a measure of the background remaining after cutting at $\lambda = 0$. In order to correctly normalize the λ-distributions of $q\bar{q}$-Monte Carlo events to those of real data, the original multiplicity distribution has to be known in advance. Therefore, the background to each event class was determined in an iterative way.

We define the observed charged-particle multiplicity m of an event as the number of tracks which have an opening angle θ with respect to the beam axis such that $|\cos\theta| < 0.92$ and a transverse momentum of larger than 40 MeV/c. Furthermore, tracks are only counted if they originate from the main vertex or from a secondary vertex consistent with a $\Lambda \to p\pi^-$ or a $K_S^0 \to \pi^+\pi^-$ decay.

A multiplicity distribution can be described by a vector $\vec{f}$ with components f_m denoting the number of events with the observed multiplicity m. The distribution $\vec{f}^{off}$ corresponds to the continuum data sample; $\vec{f}^{on}$is the sum of $\vec{f}^{B\overline{B}}$ and $\vec{f}^{con}$, where $\vec{f}^{B\overline{B}}$ and $\vec{f}^{con}$ are the multiplicity distributions for pure $\Upsilon(4S) \rightarrow B\overline{B}$ decays and for the continuum process $e^+e^- \rightarrow q\overline{q} \rightarrow hadrons$ at the centre-of-mass energy of the $\Upsilon(4S)$ resonance, respectively. Assuming that the shape of the multiplicity distribution of continuum events remains unaffected by a shift of 100 MeV in the centre-of-mass energy, we obtain $\vec{f}^{B\overline{B}}$ by subtracting the scaled multiplicity distribution of our continuum data from the observed distribution $\vec{f}^{on}$. The scaling factor accounts for the ratio of the integrated luminosities of the $\Upsilon(4S)$ and the continuum data sample and for the energy dependence of the hadronic continuum cross-section.

4.2 The Unfolding Procedure

To extract the *original* charged-particle multiplicity distribution $\vec{F}$ from the *observed* multiplicity distribution $\vec{f}$, we have to apply an unfolding method which accounts for detection inefficiencies and particle loss. The components F_n and f_m of the vectors $\vec{F}$ and $\vec{f}$ count the number of events which were produced with n ($n = 0, 2, 4, ..., n_{max}$) charged particles and are observed as m-prong events ($m = 0, 1, 2, \ldots, m_{max}$), respectively. Detection inefficiencies cause m to take even and odd values. Furthermore, photon conversion to e^+e^- pairs can increase the number of charged particles in an event so that m can even be larger than n. We use the equation

$$f_m = \sum_{n=0}^{n_{max}} A_{mn} F_n \qquad (m = 0, 1, 2, \ldots, m_{max}) \tag{6}$$

to relate the numbers of observed m-prong events to the numbers of events with an original charged-particle multiplicity n. An element A_{mn} of the $m \times n$ matrix $\mathbf{A}$ denotes the probability that an event with original multiplicity n is observed as m-prong event.

To obtain the original multiplicity distribution $\vec{F}$ one has to calculate the matrix $\mathbf{A}$ by means of Monte Carlo techniques. An element of the acceptance matrix $\mathbf{A}$ is determined from the number of Monte Carlo events M_{mn}, which were generated with n charged particles and observed as m-prong events, divided by the total number F_n^{MC} of generated events with multiplicity n:

$$A_{mn} = \frac{M_{mn}}{F_n^{MC}} \, . \tag{7}$$

Note that the matrix elements of $\mathbf{A}$ are independent of the shape of the multiplicity distribution used in the Monte Carlo generator.

The original multiplicity distribution is then obtained from the observed one by minimizing the χ^2-function

$$\chi^2 = \sum_{m \geq 0} \left(\frac{f_m - \sum_n (A_{mn} F_n)}{\sigma_m} \right)^2 \, . \tag{8}$$

Here σ_m is the statistical error on the number of observed m-prong events.

The acceptances A_{mn} for continuum events and $\Upsilon(4S) \rightarrow B\overline{B}$ decays were calculated from Monte Carlo event samples generated according to the LUND model [5]. In case of $B\overline{B}$ events, the LUND Monte Carlo was modified to account for the known branching ratios of B-decays. To determine the acceptances A_{mn} the generated events were propagated through a complete detector simulation and analyzed with the same selection criteria as real data. We note that our definition of the original multiplicity includes charged particles from $K_S^0 \rightarrow \pi^+\pi^-$ and $\Lambda \rightarrow p\pi^-$ decays, whereas those from K_L^0 decays are excluded. This definition is consistent with most experiments.

A known feature of such unfolding procedures is that small statistical fluctuations in the Monte Carlo generated matrix $\mathbf{M}$ of eq. 7 are propagated into large fluctuations of the unfolded distribution [13]. Hence, unfolding the same distribution with two acceptance matrices derived from independent Monte Carlo event samples results in unfolded distributions which differ considerably for a point-to-point comparison but are statistically equivalent if the correlations between different data points are taken into account.

To avoid the very time-consuming Monte Carlo generation with complete detector simulation of large event samples, we use the following procedure to estimate the effect of limited Monte Carlo statistics. From a Monte Carlo sample of about 60 000 events we determine the matrix M_{mn} and calculate the acceptances A_{mn}. The effect of limited Monte Carlo statistics is studied by first forming the probabilities $P_{mn} = \sum_{i=0}^{m} \mathbf{A}_{in}$ to observe at most m tracks in an event of charged-particle multiplicity n. For each value n we then choose a set of random numbers $S_n := \{ w_{ni} : 1 \leq i \leq F_n^{MC} \}$, where the numbers w_{ni} are uniformly distributed in the interval $[0, 1]$. A new matrix $\mathbf{M}'$ with elements M'_{mn} is obtained by counting how often a random number $w \in S_n$ falls in the interval $P_{m-1,n} \leq w < P_{mn}$. As a result the new matrix M'_{mn} and the corresponding acceptances A'_{mn} differ from the original ones but are equal within statistics. Repeating this procedure many times and unfolding the measured multiplicity distribution f_m with each acceptance matrix A'_{mn} allows one to study the effect of the limited Monte Carlo statistics on the unfolded distribution.

For the continuum and $\Upsilon(4S)$ data we show in Fig. 5 the resulting unfolded distributions of the charged-particle multiplicity after repeating this procedure 500 times. The unfolded multiplicity distributions are recorded for each n in histograms (drawn vertically). The individual F_n's for fixed n scatter with a gaussian distribution around their mean values $\overline{F_n}$ with root-mean-squares, which reflect the systematic uncertainty of the unfolding procedure due to the limited Monte Carlo statistics. In contrast to the multi-

plicity distribution obtained from a particular acceptance matrix **A** the mean values $\overline{F_n}$ follow a smooth distribution.

Finally, we multiply for each multiplicity n the value $\overline{F_n}$ by a factor r_n to account for radiative corrections. The factors r_n were derived from Monte Carlo simulations by comparing the multiplicity distributions generated with and without initial photon radiation.

4.3 Results on Charged-Particle Multiplicity

In Fig. 6 the measured multiplicity distributions of the continuum and $\Upsilon(4S)$ data are shown as histograms. The unfolded distributions were obtained by restricting the unfolding procedure to certain multiplicity ranges, e.g. $6 \leq n \leq 18$ or $2 \leq n \leq 22$, which are the narrowest and widest intervals we used. When neccessary, the values for the lower and higher multiplicities were estimated on the assumption that their relative fractions are the same as in the generated Monte Carlo sample, e.g. for a unfolding range of $4 \leq n \leq 20$ we fix the ratios $F_0 : F_2 : F_4$ and $F_{20} : F_{22}$ according to the Monte Carlo distributions. In Fig. 6 the average of the resulting distributions for the different multiplicity ranges for continuum and $\Upsilon(4S)$ data are displayed as dots with error bars. The corresponding variations reflect the uncertainty in obtaining the low and high multiplicities of the charged multiplicity distributions and contribute 0.2% to the systematic error of the mean charged multiplicty for both continuum and $\Upsilon(4S)$. In Tab. 2 we give the values of the unfolded multiplicity distributions. Also given are the mean charged-particle multiplicity $\langle n_{ch} \rangle$, the dispersion D, and the leading moments $C_k = \langle n_{ch}^k \rangle / \langle n_{ch} \rangle^k$ of the distributions. The statistical errors are derived from the full covariance matrix. In addition to the contribution mentioned above the systematic errors take into account the uncertainties in the background subtraction (0.4% on $\langle n_{ch} \rangle_{cont.}$), the corrections for K_S^0 and Λ decays and for charged tracks due to photon conversion (1.2% on $\langle n_{ch} \rangle_{cont./\Upsilon(4S)}$), and a 1.5% error on the drift chamber efficiency (1.9/1.8% on $\langle n_{ch} \rangle_{cont./\Upsilon(4S)}$). Furthermore, they cover the statistical uncertainties of the acceptance matrix (0.4/0.3% on $\langle n_{ch} \rangle_{cont./\Upsilon(4S)}$). For the multiplicity distribution of $B\overline{B}$-events, the systematic errors also include the uncertainties in the continuum subtraction (0.4% on $\langle n_{ch} \rangle_{\Upsilon(4S)}$). An estimate of the systematic error of the radiative correction for the continuum data was obtained by including and excluding resonances at low s in the Monte Carlo generation (0.4% on $\langle n_{ch} \rangle_{cont.}$).

Our result for the mean multiplicity of continuum events of $\langle n_{ch} \rangle_{cont} = 8.35 \pm 0.02 \pm 0.20$ at a centre-of-mass energy of 10.47 GeV is in good agreement with those published by other experiments for similar centre-of-mass energies [14].

For $\Upsilon(4S) \to B\overline{B}$ decays we obtain a value of $\langle n_{ch} \rangle_{\Upsilon(4S)} = 10.81 \pm 0.05 \pm 0.23$ which corresponds to an average production of 5.4 charged particles per B-meson decay. Our measurement is in good agreement with the CLEO result [15] of $\langle n_{ch} \rangle_{\Upsilon(4S)} = 10.99 \pm 0.06 \pm$

0.29.

In Tab. 3 we list the mean multiplicity $\langle n_{ch} \rangle$ and the dispersion D of the used Monte Carlo event generators. As already pointed out, our derived multiplicity distributions are independent of the multiplicity distribution assumed in the Monte Carlo generators. Comparing the moments listed in Tab. 3 for the LUND Monte Carlo to those of the real data in Tab. 2, we conclude that the Monte Carlo reproduces the data within errors.

5 Summary

We have determined the R value in non-resonant e^+e^- annihilation at a centre-of-mass energy of 9.36 GeV. Although our measured R value is the most precise one compared to previous results of various experiments at similar centre-of-mass energies, its systematic error is still too large to allow an accurate determination of the strong coupling constant α_s and the QCD scaling parameter $\Lambda_{\overline{MS}}$.

We have also measured the mean charged-particle multiplicity $\langle n_{ch} \rangle$ and the dispersion D of the multiplicity distribution for $\Upsilon(4S) \to B\overline{B}$ decays and for $q\overline{q}$ continuum events at centre-of-mass energies just below the $B\overline{B}$ threshold. Our results are in good agreement with results obtained by other e^+e^- experiments for $\Upsilon(4S)$ decays and non-resonant e^+e^- annihilation at similar centre-of-mass energies.

Acknowledgement

It is a pleasure to thank U. Djuanda, E. Konrad, E. Michel, and W. Reinsch for their competent technical help in running the experiment and processing the data. We thank Dr. H. Nesemann, B. Sarau, and the DORIS group for the excellent operation of the storage ring. The visiting groups wish to thank the DESY directorate for the support and kind hospitality extended to them.

References

[1] S. G. Gorishny *et al.*, Phys. Lett. B212 (1988) 238

[2] S. G. Gorishny *et al.*, Phys. Lett. B256 (1991) 81

[3] C. Hast (ARGUS Collab.), Diploma Thesis, Univ. Dortmund (1988)

[4] H. Albrecht *et al.* (ARGUS Collab.), Nucl. Instr. Meth. A275 (1989) 1

[5] T. Sjöstrand: Comp. Phys. Comm. 39 (1986) 347;
T. Sjöstrand and M. Bengtsson: Comp. Phys. Comm. 43 (1987) 367

[6] L. Crigee and G. Knies (PLUTO Collab.), Phys. Rep. C83 (1982) 151

[7] H. Albrecht *et al.* (DASP II Collab.), Phys. Lett. 116B (1982) 383

[8] P. Bock *et al.* (DESY-Heidelberg Collab.), Z. Phys. C6 (1980) 125

[9] B. Niczyporuk *et al.* (LENA Collab.), Z. Phys. C15 (1982) 299

[10] E. Rice *et al.* (CUSB Collab.), Phys. Rev. Lett. 48 (1982) 906

[11] R. Giles *et al.* (CLEO Collab.), Phys. Rev. D29 (1984) 1285

[12] Z. Jakubowski *et al.* (Crystal Ball Collab.), Z. Phys. C40 (1988) 49

[13] V. Blobel, DESY 84-118, published in CERN Comp. School 1984, 88

[14] P. Mättig, Phys. Rep. 177 (1989) 141

[15] B. Gittelman, S. Stone, *B* Meson Decay, published in A. Ali, P. Söding (editors), High Energy Electron-Positron Physics, World Scientific Publishing Co Pte Ltd, (1988) 273

Table 1: Compilation of R measurements of various experiments at centre-of-mass energies near 10 GeV.

Experiment	$\sqrt{s}$ [GeV]	R
PLUTO [6]	9.4	$3.67 \pm 0.23 \pm 0.29$
DASP II [7]	9.5	$3.73 \pm 0.16 \pm 0.28$
DESY-Heidelberg [8]	9.4	$3.80 \pm 0.27 \pm 0.42$
LENA [9]	9.1 - 9.5	$3.34 \pm 0.09 \pm 0.18$
CUSB [10]	10.4	$3.54 \pm 0.05 \pm 0.40$
CLEO [11]	10.4	$3.77 \pm 0.06 \pm 0.24$
Crystal Ball [12]	9.4	$3.48 \pm 0.04 \pm 0.16$
ARGUS (this work)	9.36	$3.46 \pm 0.03 \pm 0.13$
weighted average	≈ 10	3.51 ± 0.08

Table 2: Unfolded charged-particle multiplicity distribution together with the mean charged-particle multiplicity $\langle n_{ch} \rangle$, the dispersion D, the ratio $\langle n_{ch} \rangle / D$, and higher moments $C_k = \langle n_{ch}^k \rangle / \langle n_{ch} \rangle^k$ for $\Upsilon(4S) \to B\overline{B}$ decays and continuum events, respectively. The statistical errors are derived from the covariance matrix.

	$\Upsilon(4S) \to B\overline{B}$	Continuum
n	fraction of n-prong events in %	
2		$1.1 \pm 0.1 \pm 0.2$
4	$0.8 \pm 0.7 \pm 0.7$	$8.6 \pm 0.2 \pm 0.7$
6	$8.8 \pm 1.5 \pm 1.6$	$22.4 \pm 0.4 \pm 1.2$
8	$18.8 \pm 2.4 \pm 2.7$	$29.2 \pm 0.7 \pm 1.9$
10	$26.7 \pm 3.3 \pm 3.9$	$22.9 \pm 1.1 \pm 1.7$
12	$23.0 \pm 3.6 \pm 4.8$	$10.8 \pm 1.1 \pm 1.8$
14	$13.2 \pm 2.8 \pm 4.5$	$3.8 \pm 0.7 \pm 2.3$
16	$5.9 \pm 1.9 \pm 3.2$	$0.9 \pm 0.8 \pm 1.7$
18	$2.6 \pm 1.3 \pm 2.7$	$0.2 \pm 0.8 \pm 1.0$
20	$0.2 \pm 0.2 \pm 1.0$	
$\langle n_{ch} \rangle$	$10.81 \pm 0.05 \pm 0.23$	$8.35 \pm 0.02 \pm 0.20$
D	$2.98 \pm 0.04 \pm 0.12$	$2.71 \pm 0.02 \pm 0.10$
$\langle n_{ch} \rangle / D$	$3.63 \pm 0.06 \pm 0.14$	$3.08 \pm 0.02 \pm 0.09$
C_2	$1.08 \pm 0.01 \pm 0.01$	$1.11 \pm 0.01 \pm 0.01$
C_3	$1.24 \pm 0.01 \pm 0.02$	$1.33 \pm 0.01 \pm 0.03$
C_4	$1.50 \pm 0.02 \pm 0.04$	$1.71 \pm 0.02 \pm 0.09$
C_5	$1.91 \pm 0.04 \pm 0.09$	$2.34 \pm 0.06 \pm 0.25$

Table 3: The mean charged-particle multiplicity $\langle n_{ch} \rangle$ and the dispersion D of the Monte Carlo generated multiplicity distributions to simulate $\Upsilon(4S) \to B\overline{B}$ and continuum events, respectively.

	$\Upsilon(4S) \to B\overline{B}$ Monte Carlo	$q\overline{q}$ Monte Carlo (LUND 6.2)
$\langle n_{ch} \rangle$	10.74 ± 0.02	8.25 ± 0.01
D	2.86 ± 0.01	2.52 ± 0.01

Figure Captions

Fig. 1: Scatter plot of the scaled sum of the observed shower energy of the two particles with the largest momenta $E_{12}/\sqrt{s}$ versus $\cos\alpha$, where α is the isolated-track-angle described in the text. The dots are data taken in the continuum. The applied cut is indicated by the solid line and rejects radiative Bhabha events which populate the lower-right region of the plot.

Fig. 2: Scatter plot of the sum of the particle momenta along the beam axis $P_z = \sum p_z/\sqrt{s}$ versus the total momentum sum $P_{sum} = \sum |p|/\sqrt{s}$ for a continuum event sample. The applied cut is indicated by the solid line and rejects mainly two-photon, beam-gas and beam-wall events, which dominate the region below the line.

Fig. 3: Scatter plot of thrust versus the $\cos\alpha_{ch}$, where α_{ch} is the isolated-track-angle described in the text. The dots are data taken in the continuum. The applied cut is indicated by the solid line and rejects τ-pair events which populate the right part of the plot.

Fig. 4: The distribution of the parameter $\lambda = P_{sum} - 0.3 - 2.5 \cdot (P_z)^2$ for events of observed multiplicity $m = 4$ of the continuum data (crosses) and the $q\overline{q}$ Monte Carlo data (hatched histogram). Events with $\lambda > 0$ are accepted.

Fig. 5: The effect of statistical uncertainties in the Monte Carlo generated acceptance matrix **A** on the unfolded multiplicity distributions; **a)** continuum data and **b)** $\Upsilon(4S)$ data. The vertically drawn histograms indicate the variations in the result of the unfolding procedure due to the limited Monte Carlo statistics. The mean values $\overline{F_n}$ are drawn as filled circles. Their statistical errors are shown as error bars and are derived from the statistical uncertainties of the measured multiplicity distributions.

Fig. 6: The histograms show the measured multiplicity distributions for **a)** continuum events and **b)** $\Upsilon(4S) \to B\overline{B}$ events. The unfolded distributions are marked by filled circles with error bars.

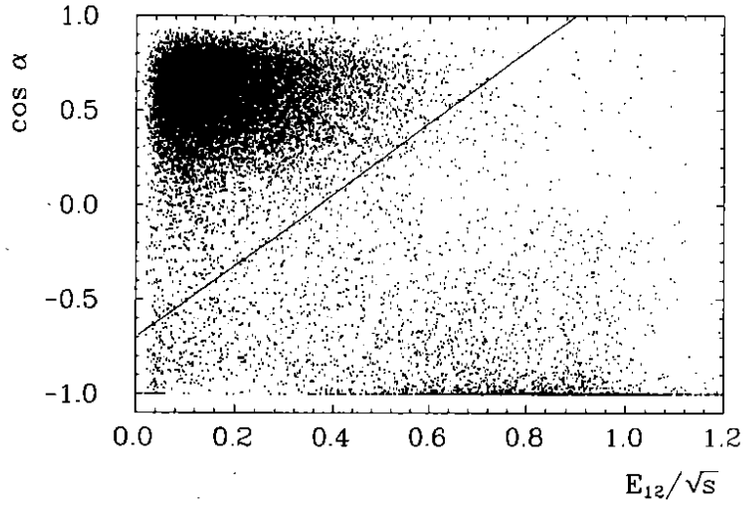
cos α
1.0
0.5
0.0
-0.5
-1.0
0.0
0.2
0.4
0.6
0.8
1.0
1.2
E12/√s

Fig. 1

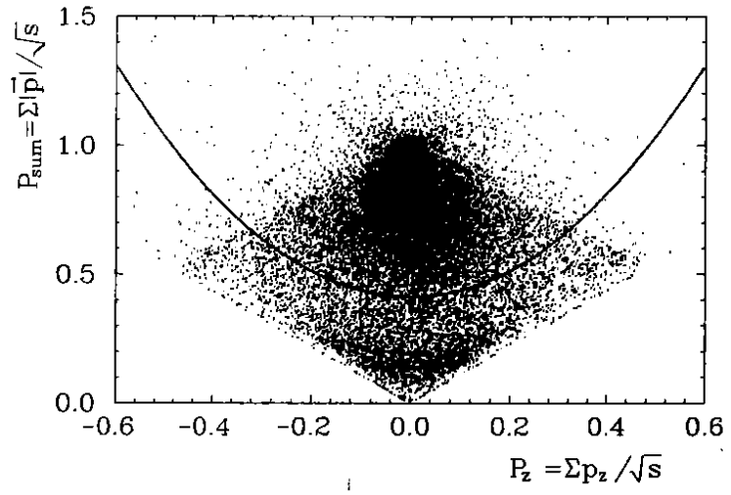
Psum=Σ|p|/√s
1.5
1.0
0.5
0.0
-0.6
-0.4
-0.2
0.0
0.2
0.4
0.6
Pz =Σpz /√s

Fig. 2

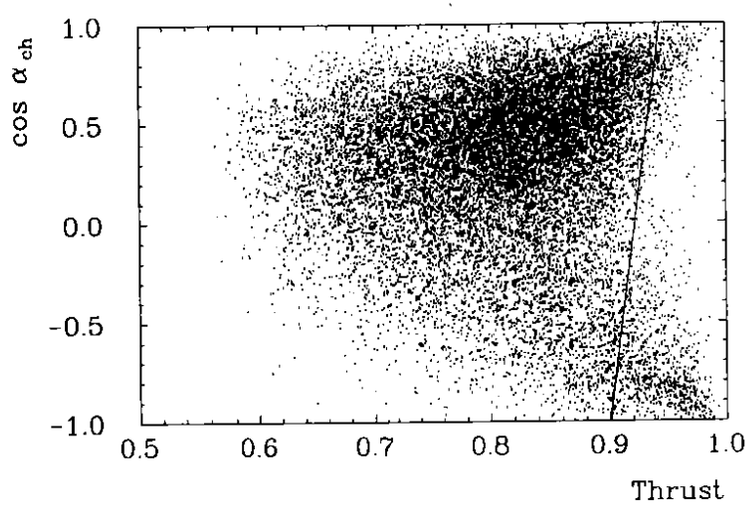
cos α_{ch}
1.0
0.5
0.0
-0.5
-1.0
0.5
0.6
0.7
0.8
0.9
1.0
Thrust

Fig. 3

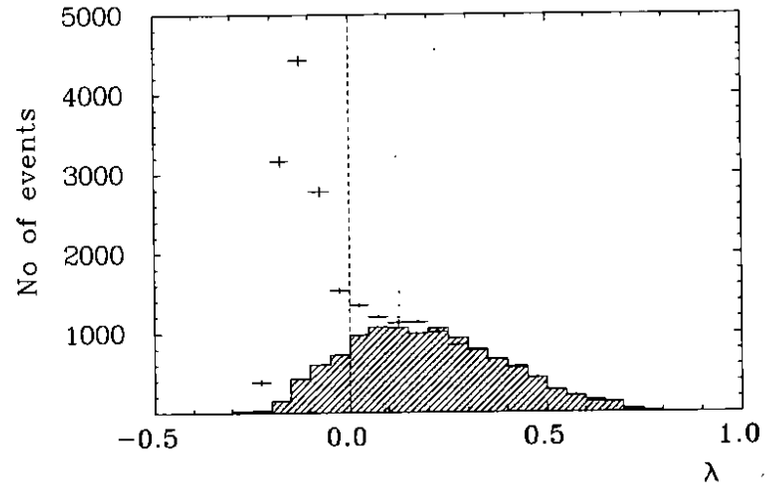
No of events
5000
4000
3000
2000
1000
−0.5
0.0
0.5
1.0
λ

Fig. 4

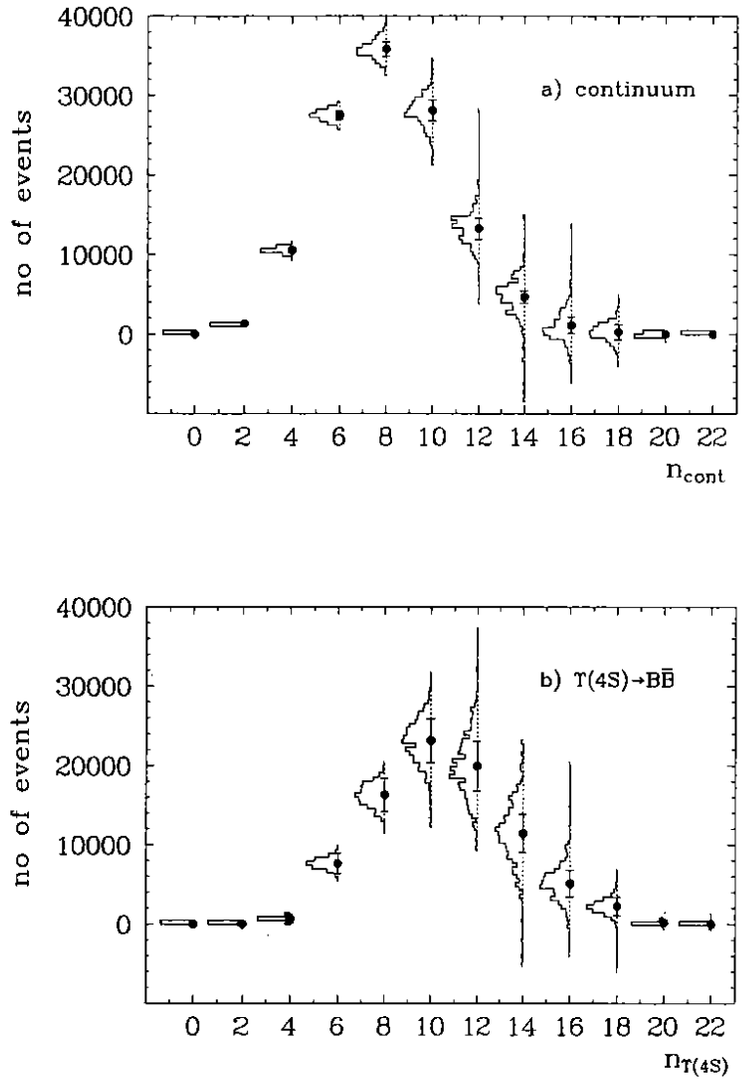
a) continuum
b) Υ(4S)→BB̄
no of events
n_{cont}
$n_{\Upsilon(4S)}$

Fig. 5

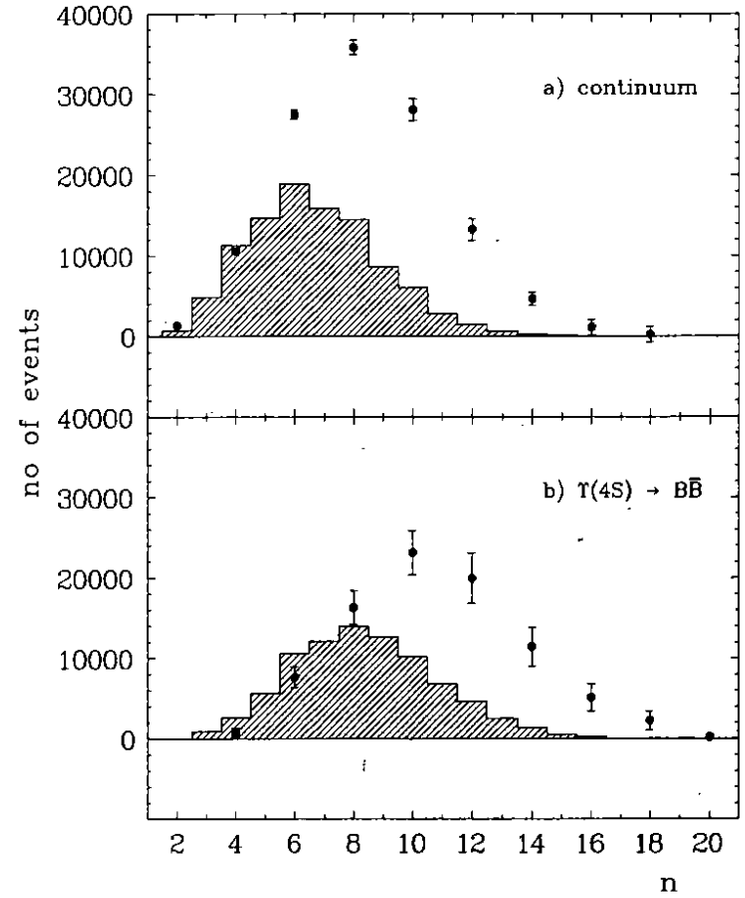
a) continuum
b) Υ(4S) → BB̄
no of events
n

Fig. 6